Subgrade Reaction Characteristics to the Anchor Pile of a Sheet Pile Quay Wall

Kenichiro Miyashita
Pacific Consultants Co. Ltd, Japan
kenichirou.miyashita@os.pacific.co.jp (corresponding author)

Takashi Nagao
Kobe University, Japan
nagao@people.kobe-u.ac.jp

Received: 5 October 2023 | Revised: 19 December 2023 and 15 January 2024 | Accepted: 16 January 2024

 DOI: https://doi.org/10.48084/etasr.6474

ABSTRACT

The Conventional Design Method (CDM) for anchored sheet pile quay walls cannot accurately calculate the anchor pile deformation, partly because it does not properly consider the subgrade reaction. This study aims to clarify the subgrade reaction characteristics to the anchor pile using finite element analysis. The CDM assumes that passive failure occurs at the front of the anchor pile. On the contrary, this study shows that the active failure region generated from the back of the sheet pile wall expands to the periphery of the anchor pile and the passive failure region is not generated at its front. Thus, the subgrade reaction to the anchor pile is found to be smaller than the CDM assumption. The CDM also neglects the subgrade reaction in parts shallower than the tie-rod mounting height in the pile front. This study clarifies that the subgrade reaction in this part greatly contributes to the deformation resistance of the pile. Consequently, the subgrade reaction in the shallower range than the tie-rod mounting height is greater than or equal to that in the deeper range. Furthermore, the subgrade reaction has a lower upper limit when acting on the anchor pile than when acting on a horizontally stratified ground, and the difference between these limits widens as the reference earthquake strengthens.

Keywords-sheet pile quay wall; seismic resistant design; subgrade reaction; anchor pile; active failure

I. INTRODUCTION

Quay walls are essential port facilities for cargo handling. During an earthquake, quay walls can deform even if their structural members are sound, causing serviceability problems [1-3]. The amount of deformation should be assessed in the seismic design of quay walls [4-6]. In an anchored sheet pile quay wall, the sheet pile wall and the anchor pile are combined by a tie-rod. As the tie-rod is very stiff, its elongation during an earthquake is negligible, and the deformation at the crown height of the sheet pile quay wall coincides with that of the anchor pile. In this scenario, the deformation of the anchor pile must be calculated accurately.

The deformation of the anchor pile during an earthquake is greatly influenced by its interaction with the ground. Various methods have been proposed to simply evaluate the deformation of anchor piles during earthquakes based on the assumption that the ground deforms as a rigid body block [7-9]. However, these methods cannot calculate the amount of deformation with good accuracy due to insufficient consideration of the interaction between the anchor pile and the ground. The Conventional Design Method (CDM) [5] uses the beam-on-Winkler-foundation method, which considers the interaction between the anchor pile and the ground to calculate its deformation during earthquakes. However, the CDM cannot also accurately evaluate the deformation of the anchor pile during an earthquake for two reasons [10]. First, the anchor pile is subjected to translation, rotation, and bending deformations during an earthquake, whereas the CDM assumes that the anchor pile is not deformed below a certain depth, at which it is strongly confined and deformed only by bending at shallower depths. In practice, the ground behind the sheet pile wall is not horizontally stratified and experiences shear stress prior to the occurrence of the earthquake. Therefore, the earthquake causes residual deformation in the ground, resulting in kinematic forces that generate translations and rotations in the anchor pile. In [11], a simple and accurate method was presented to estimate the deformation of anchor piles caused by translation and rotation. Second, CDM cannot properly evaluate the subgrade reaction properties that greatly contribute to the bending deformation resistance of piles because it assumes that the anchor piles are embedded in horizontally stratified ground. Consequently, the bending deformation is poorly estimated [11]. Several studies have reported the subgrade reaction to piles in horizontally stratified [12-14] and sloping grounds [15-17]. Other studies have investigated the front ground of an independent pile installed behind a sheet pile wall [18]. However, the subgrade reaction characteristics of the anchor pile behind the sheet pile wall have not been reported.

This study aims to investigate the subgrade reaction properties of the ground in front of an anchor pile using Finite Element Analysis (FEA) to improve the accuracy in calculating the bending deformation of piles. At first, the Subgrade Reaction Modulus (SRM) obtained through the FEA was compared with that of the CDM. The difference between the subgrade reaction properties of the ground in front of the anchor pile and horizontally stratified ground was then clarified. Finally, it is shown that this difference increases with the increasing strength of a reference earthquake.

II. METHOD

This study considered two cross-sections at different water depths, -5.5 and -11.0 m [11], designed by the CDM, as shown in Figure 1. The elevation of the ground surface was 4.0 m. The anchor pile positions were 13.5 m and 18.9 m from the sheet pile wall, respectively. CDM considers the subgrade reaction under tension of the tie-rod and deformation of the pile. The bending moment generated in the pile was obtained by solving the following differential equation:

$$EI\frac{d^4u}{dy^4} = -Bp \quad (1)$$

where EI is the flexural rigidity of the pile, u is the lateral displacement of the pile at depth y, p is the subgrade reaction, and B is the pile width. The nonlinear load-displacement relationship of a pile often considers the nonlinear characteristics of the soil [19-21]. Based on the experimental results, the CDM calculates the subgrade reaction p as follows [5]:

$$p = k_c u^{0.5} \quad (2)$$

where k_c is the SRM. The SRM is often considered to depend on the foundation width [22-23], but this dependence is ignored when designing anchor piles [5].

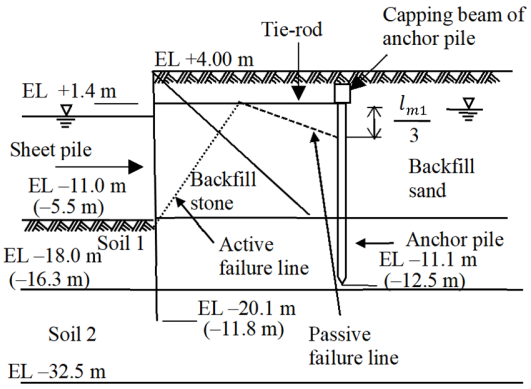

Fig. 1. Profile of the sheet pile quay wall in this study. Values at a water depth of -5.5 m are given in parentheses and EL denotes elevation.

This study adopts the FEA code used in [11], namely the FLIP code [24], which is widely used to evaluate seismic responses of port facilities. Previous studies reported that the FLIP code accurately reproduces the residual deformation of the damaged sheet pile quay walls by earthquakes and the experimental results of the models [25-27]. The ground conditions, structural members, boundary conditions between members and the ground, and earthquake ground motions were set to those in [11]. Viscos boundaries were applied to the bottom and side. A bilinear joint element was applied to the boundary between the wall and soil to consider wall friction. The interaction between the anchor pile and the ground was considered using the soil-spring element [28], which can take into account the three-dimensional effect. The stress-strain relationship of the ground is expressed by a nonlinear relationship based on the hyperbolic model [29] using the multispring element [30]. The hyperbolic model shows a substantial damping coefficient compared to the experimental result in the large shear strain range. Thus, the FLIP code modifies the hysteresis curve to reduce the area of the hysteresis loop compared to that given by the Masing rule [31] to prevent the damping coefficient from exceeding the maximum value [32]. Detailed equations for the hyperbolic model are given in [11]. The effects of liquefaction were neglected. Tables I and II show the ground conditions and dimensions of the structural members, respectively. The natural period of the ground was set to 0.8 s for both ground conditions, based on the values typically observed in the field.

TABLE I. GROUND CONDITIONS

Soil	ρ (t/m^3)	G_{ma} (kN/m^2)	σ'_{ma} (kN/m^2)	ϕ (°)
Backfill sand	2.0	58,300	89.8	38
Soil 1	2.0	72,200	198.5	39
Soil 2	2.0	125,000	279.2	39
Backfill stone	2.0	101,250	98	40
Wall friction angle (°)	In front of the wall: $\delta = 15$ Behind the wall: $\delta = 0$			
Common physical properties	$h_{max} = 0.24$, $K_w = 2{,}200{,}000$ kN/m^2 $\nu = 0.33$			

Note: ρ = saturated unit weight, G_{ma} = reference shear modulus, σ'_{ma} = reference average effective confining stress, ϕ = shear resistance angle, h_{max} = maximum damping coefficient, K_w = bulk modulus of pore water, ν = Poisson's ratio.

TABLE II. DIMENSIONS OF THE STRUCTURAL MEMBERS

Water depth (m)	Sheet pile		Tie-rod	
	Depth of embedment (m)	Moment of inertia of area (m^4/m)	Area (m^2/m)	Length (m)
–5.5	–11.8	0.000104	0.00063	13.5
–11.0	–20.1	0.000791	0.00128	18.9
Water depth (m)	**Anchor pile**			
	Pile length (m)	**Moment of inertia of area (m^4/m)**		
–5.5	14.2	0.000304		
–11.0	12.5	0.000516		

Note: Elastic modulus of all structural members is 200 kN/mm^2

As an example, Figure 2 shows a Finite Element (FE) mesh around the quay wall water depth of -5.5 m. The horizontal length of the FE model was 310 m. The height of the mesh was set at approximately 1.5 m to transmit seismic waves of up to 15 Hz. A two-step analysis was carried out. At first, a dead weight analysis was performed to evaluate the stress generated in the ground and structural members prior to the earthquake, and then a dynamic analysis was performed. Figure 3 shows the time history of the waveforms used in the calculations. The Hachinohe and Iwakuni waves have maximum accelerations of 1.0 and 1.5 m/s^2, respectively, and are dominated by low (0.4-1.5 Hz) and high frequencies (~4.0 Hz), respectively.

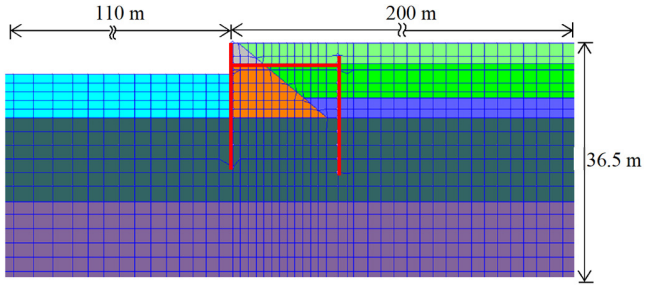

Fig. 2. FE mesh around the quay wall.

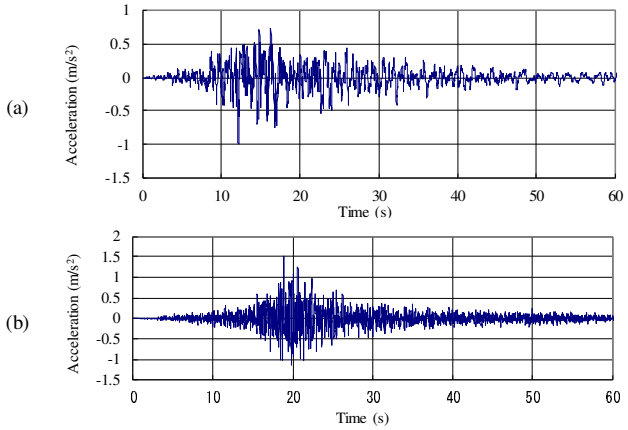

Fig. 3. Input ground motions: (a) Hachinohe wave and (b) Iwakuni wave.

III. RESULTS AND DISCUSSION

A. Bending Deformation of the Anchor Pile

Figure 4 compares the CDM- and FEA-calculated bending moments of the anchor piles after the earthquake. In both results, the bending moment increases with depth because the distance from the tie-rod tension application point becomes longer. Then, the bending moment decreases at a certain depth, since the effect of the ground resistance becomes large. Here, the bending moment in the CDM calculation uses the residual tie-rod tension determined in the FEA. Except when the cross-section of a water depth of -11 m is subjected to the Hachinohe wave, the CDM gives larger bending moment maxima of the anchor pile than FEA. In the former exceptional case, CDM and FEA give very different generation altitudes of the bending moment maxima of the anchor pile. Figure 5 shows the bending deformation of the post-earthquake anchor pile obtained by doubly integrating the pile curvature. The deformation occurs in the negative direction, indicating that the anchor pile bends toward the side of the sea. In all cases, CDM predicted that the bending deformation begins increasing at elevations around -4.0 m, while FEA predicted a deeper onset of deformation increase, near -8.0 m elevation. In addition, except in the cross-section with the Hachinohe wave at a water depth of -11 m, the bending deformations obtained by FEA gradually decreased compared to CDM in the depth direction. In other words, the bending moments are smaller in FEA, and CDM overestimates the maximum bending moment of the anchor pile. In addition, when the Hachinohe wave was applied to the cross-section of a water depth of -11 m, the quay wall deformation was highest and the bending deformation obtained by FEA was considerably large at the pile top. In this case, the bending deformation of the pile occurred from a deeper position in FEA than in CDM. Therefore, the altitude of the maximum bending moment of the anchor piles greatly differed between CDM and FEA.

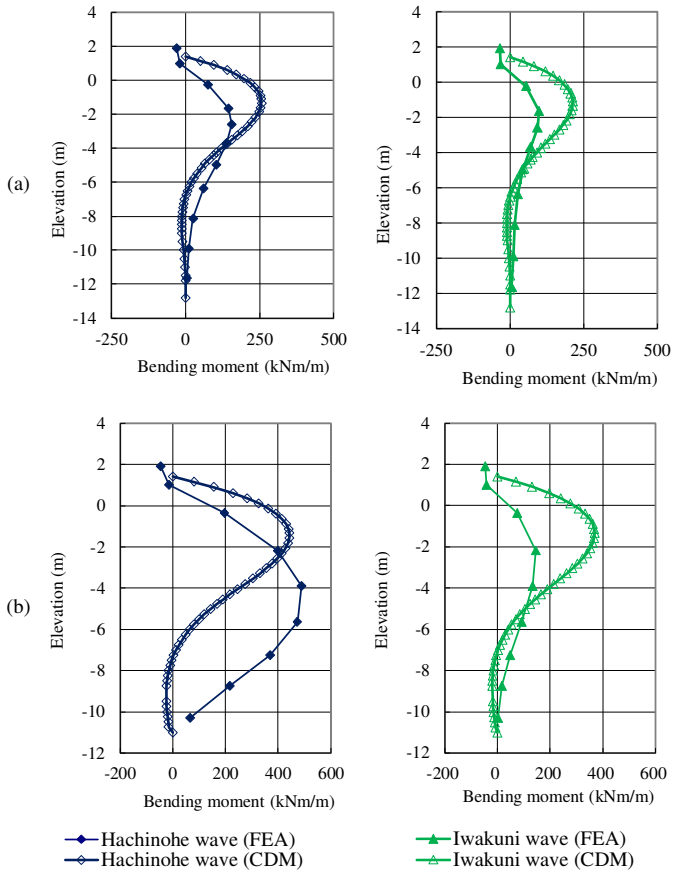

Fig. 4. Bending moments of an anchor pile obtained by the CDM and FEA: (a) at water depth -5.5 m, (b) at water depth -11 m.

B. SRM in Front of the Anchor Pile

The SRM defines the ratio of the pile subgrade reaction to the bending deformation of the pile. The SRMs were calculated in a range over which the subgrade reaction and pile-bending deformation occur in opposite directions, and their distributions are shown in Figure 6. The SRM obtained by CDM can be obtained only below the tie-rod mounting height because the CDM regards the tie-rod mounting height as the ground surface. According to the Winkler foundation model, the passive failure line is generated at $l_{m1}/3$ below the tie-rod mounting height, where l_{m1} is the depth at which the bending moment of the anchor pile first becomes zero below the tie-rod mounting height.

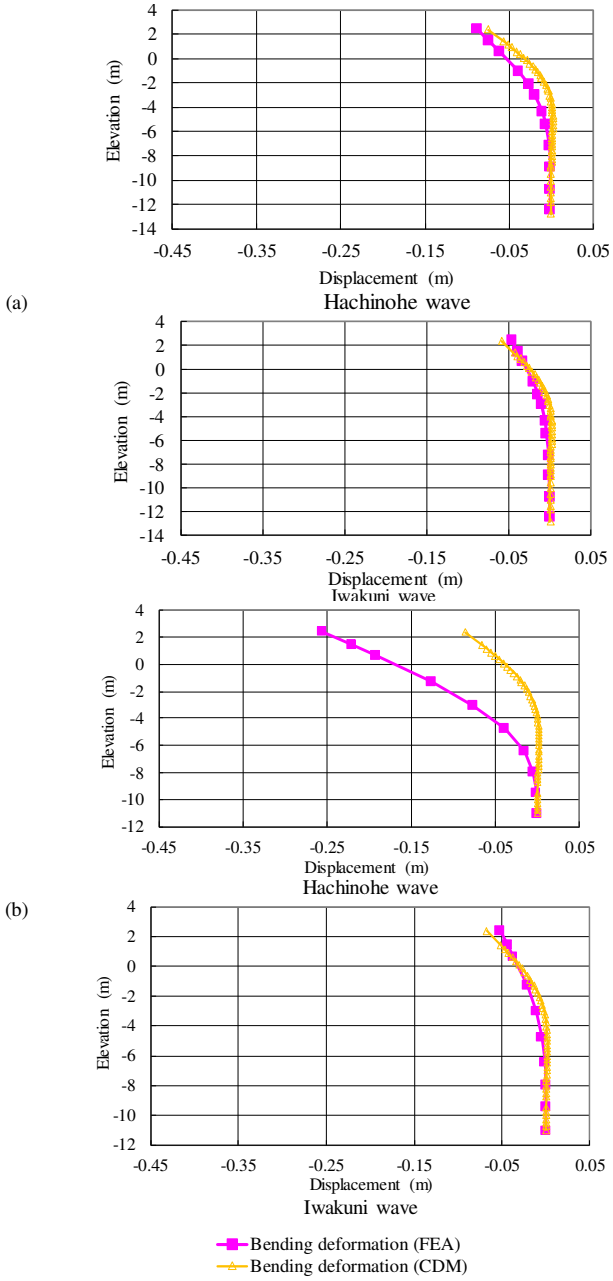

Fig. 5. Displacement of an anchor pile obtained by the CDM and FEA for water depth of (a) -5.5 m, (b) -11 m.

The SRM obtained by FEA was larger at the highest altitude than at the tie-rod mounting height and was approximately constant below the tie-rod mounting height. Conversely, the SRM obtained by CDM decreased with increasing elevation because the CDM assumes a nonlinear relationship between the subgrade reaction and the bending deformation of the pile, as in (1). Thus, the increase in the subgrade reaction becomes subdued at high bending deformations of the pile. The distributions of the SRMs also differ between the methods. The CDM gives larger SRMs than FEA, especially when the Hachinohe wave is applied to the cross-section of the -11 m water depth.

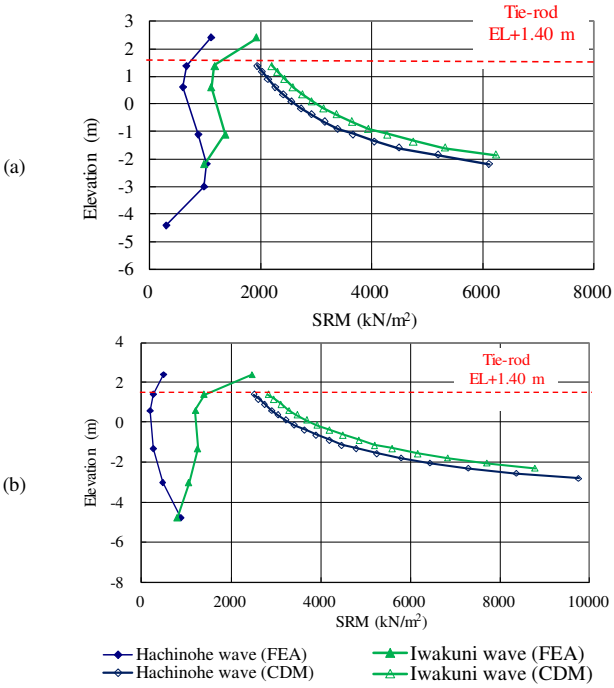

Fig. 6. SRM distribution at water depth of (a) -5.5 m, (b) -11.0 m.

C. *Causes of Differences in SRMs*

To analyze the causes of the differences in SRM between the methods, the cross-section of the -5.5 m water depth was considered with only the self-weight and a static load, as shown in Figure 7. In Case 1, the tie-rod and anchor pile were removed, leaving only the cantilever sheet pile. In Case 2, the sheet pile and the tie-rod were removed while the front area of the sheet pile was reclaimed to simulate the horizontally stratified condition. After loading a self-weight, a concentrated load of 2.5 times the tie-rod tension was applied to the pile on the landfill side at the tie-rod mounting height. To elucidate the deformation mode of the ground, the concentrated load was determined through a self-weight analysis of the cross-section in Figure 1. Case 3 is similar to Case 2, but the self-weight and stiffness of the ground in the active failure region and the reclaimed area (gray area in the figure) were set to zero when applying the concentrated load to the pile. Case 4 is the condition illustrated in Figure 7(d).

Figure 8 shows the contours of the horizontal displacements. The dashed yellow line is the boundary at which the horizontal displacement changes dramatically. Hereafter, this boundary is referred to as the pseudo-failure line. The red dashed lines indicate the active failure line behind the sheet pile and the passive failure line in front of the pile assumed by the CDM. In Case 1, the pseudo-failure line and the active failure line obtained by the CDM were similar. The deformation mode of the ground behind the cantilever sheet pile roughly agreed with the CDM assumption. In Case 2, the pseudo-failure line was similar to the active failure line at the back of the pile, and the passive failure line at the front of the pile obtained by the CDM. The deformation mode of the pile front ground also approximated the CDM assumption under the horizontally stratified condition. Unlike in Case 2, the pseudo-failure line

occurring at the front of the pile in Case 3 was horizontal until it reached the active failure region behind the sheet pile. This difference was caused by the different self-weights and ground stiffnesses in the active failure region and the reclaimed area. Cases 2 and 3 presented different horizontal displacements at the pile head, -0.026 and -0.046 m, respectively, and different levels of pile deformation. The pseudo-failure line in Case 4 resembled a smooth coupling of the pseudo-failure lines of Cases 1 and 3. An active failure region was generated just behind the sheet pile, but the passive failure region assumed by the CDM was not generated at the front of the pile because the ground was not horizontally stratified and no subgrade reaction acted on the sheet pile above the seabed level. In particular, an enlarged active failure region occurred from the back of the sheet pile to the back of the pile.

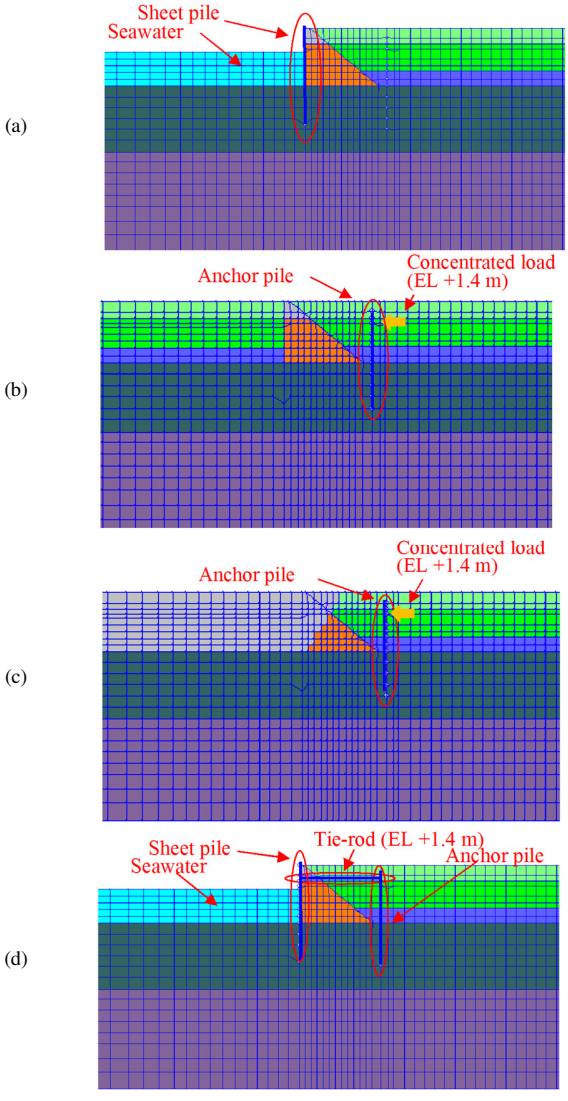

Fig. 7. Study cases for analyzing the SRM differences between the CDM and FEA methods: (a) Case 1, (b) Case 2, (c) Case 3, (d) Case 4.

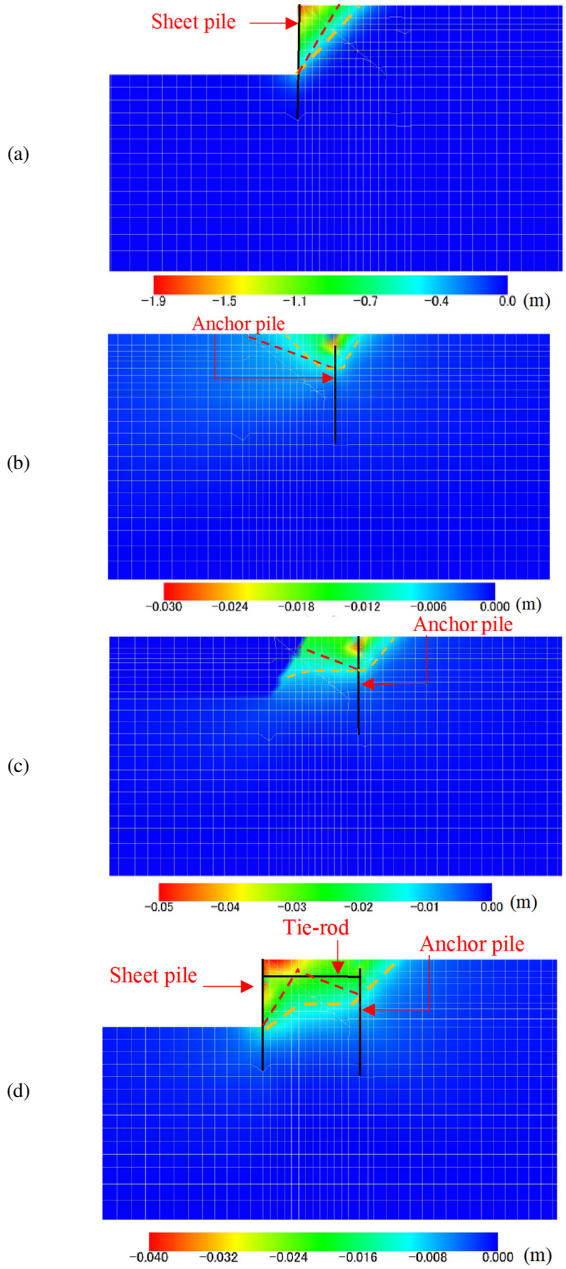

Fig. 8. Contour maps of horizontal displacements in the four cases: (a) Case 1, (b) Case 2, (c) Case 3, (d) Case 4.

The residual horizontal displacement contours were calculated for the cross-section of -11 m water depth to show the deformation mode during an earthquake (Figure 9). The red and purple dashed lines show the active and passive failure lines caused by the Monobe-Okabe seismic earth pressure [33]. The pseudo-failure (yellow dashed) line resembled that under self-weight action, the ground deformation mode during the earthquake was unchanged from that in the self-weight analysis. The pseudo-failure line was similar to the slip failure lines in [9, 34]. The FEA obtained a smaller SRM against the pile than CDM, because the pile front ground is not in a passive but in an expanded active state.

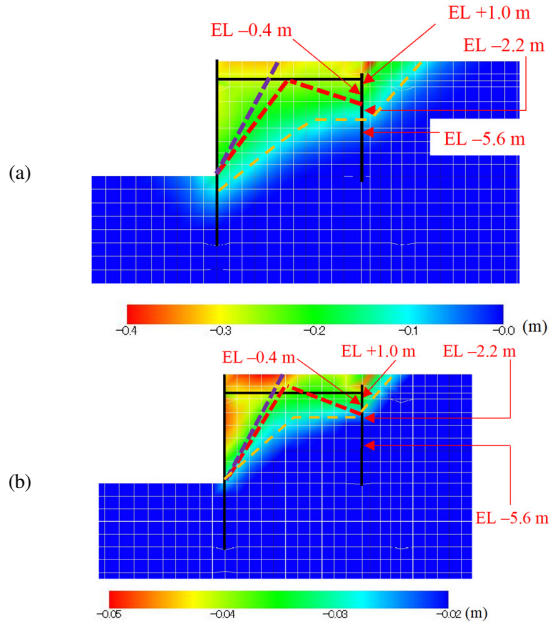

Fig. 9. Contour maps of residual horizontal displacements: (a) Hachinohe wave, (b) Iwakuni wave.

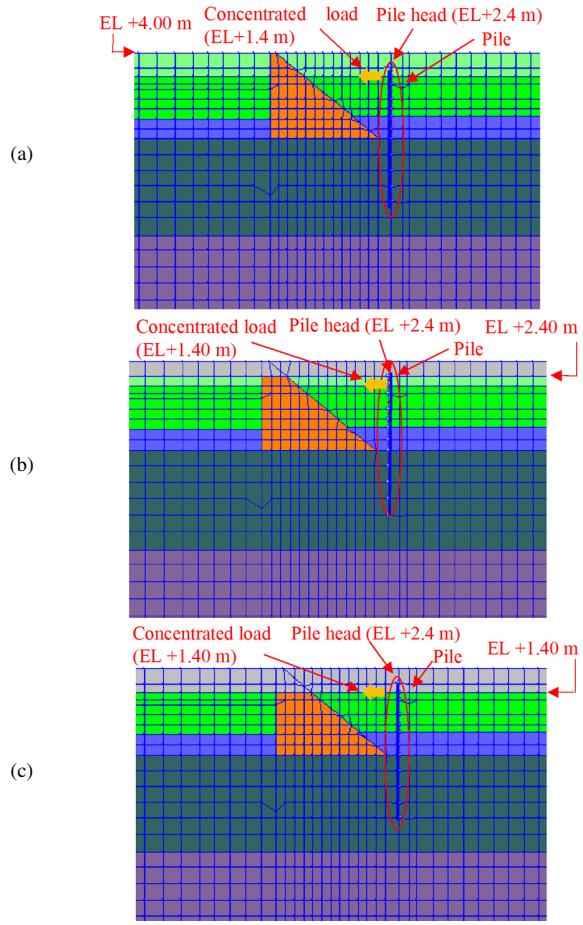

Fig. 10. Studied cases for analyzing the effect of ground height: (a) Case 1, (b) Case 2, (c) Case 3.

D. SRM Distributions

As described above, CDM assumes that the tie-rod mounting height is the ground surface although the subgrade reaction occurs above the tie-rod mounting height. Based on the cross-section of Case 2 (Figure 7), static analysis was performed for different heights of ground surface and the SRMs were compared among the cases. The concentrated load equaled the tie-rod tension obtained in the self-weight analysis. Figure 10 presents the studied cases. Case A is a basic case with constant weight and stiffness of the ground. In Case B, the weight and stiffness of the ground above the pile head (+2.4 m, gray area) were set to zero under a concentrated load. In Case C, the weight and stiffness of the ground above the concentrated load acting point (+1.4 m, gray area) were set to zero under a concentrated load. Case C accepts the CDM assumption.

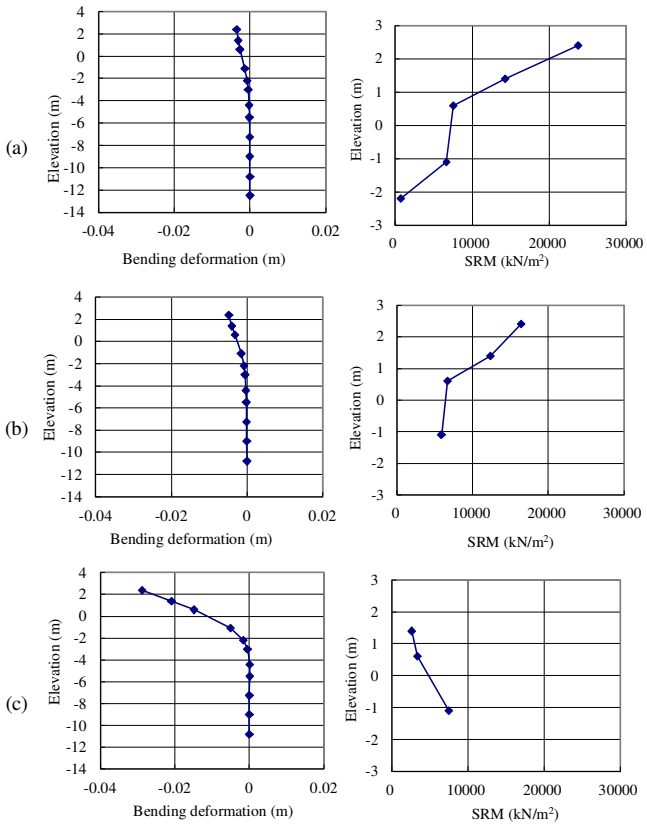

Fig. 11. Bending deformation versus SRM: (a) Case A, (b) Case B, (c) Case C.

Figure 11 shows the SRMs and bending deformations of the piles. Similarly to the results of Figure 6, the SRMs in Cases A and B at the highest altitude exceeded those at the tie-rod mounting height. In Cases A and B, the bending deformations at the pile head were 0.0035 and 0.005 m, and the SRMs at the concentrated load acting heights were 20,000 and 15,000 kN/m^2, respectively. The large pile deformation and small SRM in Case B were attributed to the zero ground weight at altitudes above the pile head under the concentrated load application. The small ground stiffness was caused by the slight

confining pressure in front of the pile. Conversely, the SRM in Case C decreased with increasing depth, in agreement with CDM (Figure 6). The bending deformation at the pile head was much larger in Case C (0.03 m) than in the other cases. The SRM at the concentrated load action height was 1,600 kN/m^2, similar to that of CDM (Figure 6(a)). The SRM distributions differ between the two methods because CDM neglects the weight and stiffness of the ground above the concentrated load-acting height.

E. Maximum Subgrade Reaction

As shown above, CDM overestimated the SRM. However, the degree of overestimation varied with the conditions, being large in the cross-section at a water depth of -11 m subjected to Hachinohe waves. Figure 12 shows the hysteretic curves of the subgrade reaction obtained by FEA and the bending deformation of the pile through the cross-section of -11 m water depth before and after the earthquake. The subgrade reaction was linearly related to bending deformation at altitudes of -5.6 m for the Hachinohe wave and -2.2 m or deeper for the Iwakuni wave. The relationship was nonlinear and asymptotically approached the upper limit at altitudes higher than the above-mentioned. The tangential SRM was calculated by connecting the points along the straight lines to the origin. Before the earthquake, the SRM at +1.9 m altitude was 5,000 kN/m^2. After the earthquake, the SRMs were 500 and 2,500 kN/m^2 for the Hachinohe and Iwakuni waves, respectively. The SRM notably decreased after the earthquake because the subgrade reaction and bending deformation are non-linearly related. By comparing Figures 9 and 12, this nonlinear relationship is observed to occur in the expanded active failure region.

In CDM, the maximum value of the subgrade reaction is set as the passive earth pressure. Table III compares the maximum subgrade reactions and the passive seismic earth pressures based on the Monobe-Okabe theory. The maximum value of the subgrade reaction in the expanded active failure region was less than the passive earth pressure, indicating that the CDM overestimates the SRM when the subgrade reaction approaches the maximum value. The Hachinohe wave enhanced the seismic intensity through the cross-section of -11 m water depth. Thus, Hachinohe waves for this water depth cross-section severely deteriorated the ground stiffness, and the extent to which the subgrade reaction reached the maximum value became the widest. Therefore, the degree of overestimation of SRM by the CDM was larger in this scenario than in the other scenarios.

TABLE III. COMPARISON OF PASSIVE EARTH PRESSURE AND MAXIMUM SUBGRADE REACTION

EL (m)	Passive earth pressure (kN/m^2)	Maximum subgrade reaction of FEA (kN/m^2)
+1.9	254	160
+1.0	316	200
–0.4	403	130
–2.2	515	120

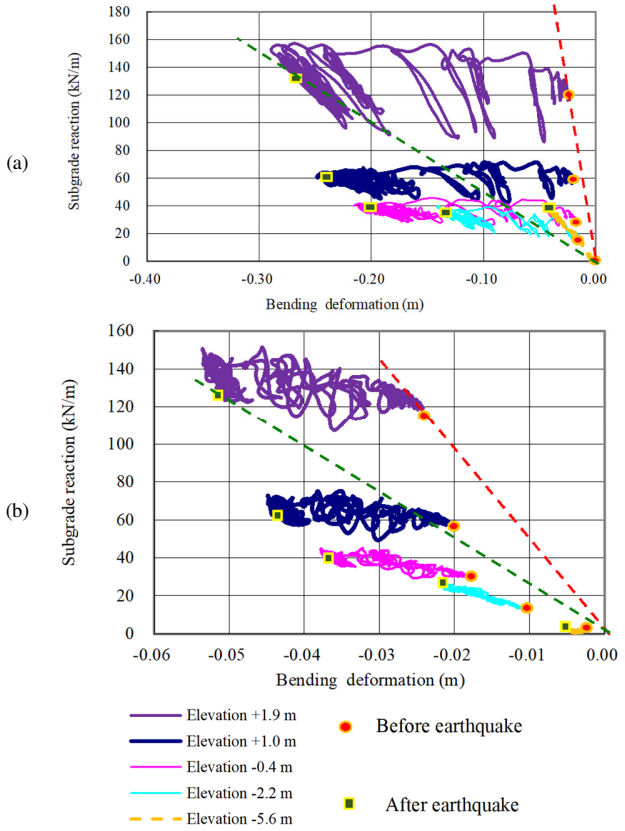

Fig. 12. Relationship between subgrade reaction and bending deformation: (a) Hachinohe wave, (b) Iwakuni wave.

IV. CONCLUSIONS

This study investigated the subgrade reaction properties of anchor piles of sheet pile quay walls using FEA. The main conclusions of the current study are:

- The subgrade reaction against the anchor pile is smaller than that of the horizontally stratified ground because the sheet pile quay wall is irregularly shaped. CDM assumes a passive state in front of the pile and, hence, overestimates the maximum subgrade reaction acting on the pile.
- CDM ignores the effects of weight and stiffness of the ground at altitudes above the tie-rod mounting height, which non-negligibly contribute to the resistance of the pile. Consequently, the subgrade reaction in the range shallower than the tie-rod mounting height is greater than or equal to that in the deeper range.
- Under the effect of active ground failure, the upper limit of the subgrade reaction is lower in the ground in front of the anchor pile than in the horizontally stratified ground. This effect is enhanced with the strengthening of the seismic motions. It should be noted that this study investigated a limited number of examination cases. Therefore, further studies should be performed on various conditions, such as different anchor pile configurations and seismic motion intensities.

REFERENCES

[1] G. A. Athanasopoulos *et al.*, "Lateral spreading of ports in the 2014 Cephalonia, Greece, earthquakes," *Soil Dynamics and Earthquake Engineering*, vol. 128, Jan. 2020, Art. no. 105874, https://doi.org/10.1016/j.soildyn.2019.105874.

[2] S. Werner *et al.*, "Seismic Performance of Port de Port-au-Prince during the Haiti Earthquake and Post-Earthquake Restoration of Cargo Throughput," *Earthquake Spectra*, vol. 27, no. 1-suppl1, pp. 387–410, 2011, https://doi.org/10.1193/1.3638716.

[3] T. Sugano, A. Nozu, E. Kohama, K. Shimosako, and Y. Kikuchi, "Damage to coastal structures," *Soils and Foundations*, vol. 54, no. 4, pp. 883–901, Aug. 2014, https://doi.org/10.1016/j.sandf.2014.06.018.

[4] "Seismic Design Guidelines for Port Structures," PIANC - International Navigation Association, Tokyo, Japan, 2001.

[5] "Technical Standards and Commentaries for Port and Harbour Facilities in Japan," The Overseas Coastal Area Development Institute of Japan, Tokyo, Japan, 2009.

[6] "EN 1998-1: Eurocode 8: Design of structures for earthquake resistance - Part 1: General rules, seismic actions and rules for buildings." 2004.

[7] R. Conti, G. M. B. Viggiani, and F. Burali D'arezzo, "Some remarks on the seismic behaviour of embedded cantilevered retaining walls," in *Geotechnical Earthquake Engineering*, ICE Publishing, 2015, pp. 137–147.

[8] L. Callisto, "On the seismic design of displacing earth retaining systems," in *Earthquake Geotechnical Engineering for Protection and Development of Environment and Constructions*, Boca Raton, FL, USA: CRC Press, 2019.

[9] C. J. W. Habets, D. J. Peters, J. G. de Gijt, A. V. Metrikine, and S. N. Jonkman, "Model Solutions for Performance-Based Seismic Analysis of an Anchored Sheet Pile Quay Wall," *International Journal of Civil and Environmental Engineering*, vol. 10, no. 3, pp. 293–305, Jan. 2016.

[10] G. Gazetas, E. Garini, and A. Zafeirakos, "Seismic analysis of tall anchored sheet-pile walls," *Soil Dynamics and Earthquake Engineering*, vol. 91, pp. 209–221, Dec. 2016, https://doi.org/10.1016/j.soildyn.2016.09.031.

[11] K. Miyashita and T. Nagao, "A Simplified Deformation Estimation Method for Anchor Piles of Sheet Pile Quay Walls under Kinematic Forces during Earthquakes," *Engineering, Technology & Applied Science Research*, vol. 13, no. 1, pp. 10108–10115, Feb. 2023, https://doi.org/10.48084/etasr.5469.

[12] M. Heidari, H. El Naggar, M. Jahanandish, and A. Ghahramani, "Generalized cyclic p–y curve modeling for analysis of laterally loaded piles," *Soil Dynamics and Earthquake Engineering*, vol. 63, pp. 138–149, Aug. 2014, https://doi.org/10.1016/j.soildyn.2014.04.001.

[13] N. Gerolymos and G. Gazetas, "Phenomenological Model Applied to Inelastic Response of Soil-Pile Interaction Systems," *Soils and Foundations*, vol. 45, no. 4, pp. 119–132, Aug. 2005, https://doi.org/10.3208/sandf.45.4_119.

[14] M. Shadlou and S. Bhattacharya, "A 1D-modelling approach for simulating the soil-pile interaction mechanism in the liquefiable ground," *Soil Dynamics and Earthquake Engineering*, vol. 158, Jul. 2022, Art. no. 107285, https://doi.org/10.1016/j.soildyn.2022.107285.

[15] K. Georgiadis and M. Georgiadis, "Undrained Lateral Pile Response in Sloping Ground," *Journal of Geotechnical and Geoenvironmental Engineering*, vol. 136, no. 11, pp. 1489–1500, Nov. 2010, https://doi.org/10.1061/(ASCE)GT.1943-5606.0000373.

[16] K. Muthukkumaran, R. Sundaravadivelu, and S. R. Gandhi, "Effect of Slope on P-Y Curves Due to Surcharge Load," *Soils and Foundations*, vol. 48, no. 3, pp. 353–361, Jun. 2008, https://doi.org/10.3208/sandf.48.353.

[17] M.-J. Hemel, M. Korff, and D. J. Peters, "Analytical model for laterally loaded pile groups in layered sloping soil," *Marine Structures*, vol. 84, Art. no. 103229, Jul. 2022, https://doi.org/10.1016/j.marstruc.2022.103229.

[18] H. Li, S. Liu, and L. Tong, "A numerical interpretation of the soil-pile interaction for the pile adjacent to an excavation in clay," *Tunnelling and Underground Space Technology*, vol. 121, Mar. 2022, Art. no. 104344, https://doi.org/10.1016/j.tust.2021.104344.

[19] H. Matlock, "Correlation for Design of Laterally Loaded Piles in Soft Clay," presented at the Offshore Technology Conference, Houston, TX, USA, Apr. 1970, https://doi.org/10.4043/1204-MS.

[20] M. Georgiadis, C. Anagnostopoulos, and S. Saflekou, "Cyclic Lateral Loading of Piles in Soft Clay," *Geotechnical Engineering*, vol. 23, no. 1, pp. 47–60, Jun. 1992.

[21] D. M. Dewaikar and D. S. Patil, "Behavior of Laterally Loaded Piles in Cohesionless Soil under One-Way Cyclic Loading," in *The New Millennium Conference*, 2001, vol. 1, pp. 97–100.

[22] T. Nagao, "Effect of Foundation Width on Subgrade Reaction Modulus," *Engineering, Technology & Applied Science Research*, vol. 10, no. 5, pp. 6253–6258, Oct. 2020, https://doi.org/10.48084/etasr.3668.

[23] T. Nagao and R. Tsutaba, "Evaluation Methods of Vertical Subgrade Reaction Modulus and Rotational Resistance Moment for Seismic Design of Embedded Foundations," *Engineering, Technology & Applied Science Research*, vol. 11, no. 4, pp. 7386–7392, Aug. 2021, https://doi.org/10.48084/etasr.4269.

[24] S. Iai, Y. Matsunaga, and T. Kameoka, "Strain Space Plasticity Model for Cyclic Mobility," *Soils and Foundations*, vol. 32, no. 2, pp. 1–15, Jun. 1992, https://doi.org/10.3208/sandf1972.32.2_1.

[25] S. Iai and T. Kameoka, "Finite Element Analysis of Earthquake Induced Damage to Anchored Sheet Pile Quay Walls," *Soils and Foundations*, vol. 33, no. 1, pp. 71–91, Mar. 1993, https://doi.org/10.3208/sandf1972.33.71.

[26] S. Higuchi *et al.*, "Evaluation of the seismic performance of dual anchored sheet pile wall," in *15th World Conference on Earthquake Engineering*, Lisbon, Portugal, 2012.

[27] T. Nagao and Y. Kurachi, "An Experimental and Analytical Study on the Seismic Performance of Piers with Different Foundation Bottom Widths," *Engineering, Technology & Applied Science Research*, vol. 12, no. 5, pp. 9142–9148, Oct. 2022, https://doi.org/10.48084/etasr.5088.

[28] O. Ozutsumi, Y. Tamari, Y. Oka, K. Ichii, S. Iai, and Y. Umeki, "Modeling of soil-pile interaction subjected to soil liquefaction in plane strain analysis," in *Proceedings of the 38th Japan National Conference on Geotechnical Engineering*, Akita, Japan, 2003, pp. 1899–1900.

[29] B. O. Hardin and V. P. Drnevich, "Shear Modulus and Damping in Soils: Design Equations and Curves," *Journal of the Soil Mechanics and Foundations Division*, vol. 98, no. 7, pp. 667–692, Jul. 1972, https://doi.org/10.1061/JSFEAQ.0001760.

[30] I. Towhata, "Modeling soil behavior under principal stress axes rotation," in *Proceedings of the 5th International Conference on Numerical Methods in Geomechanics*, Nagoya, Japan, 1985, vol. 1, pp. 523–530.

[31] G. Masing, "Eigenspannungen und verfestigung beim messing," in *Proceedings, second international congress of applied mechanics*, Zurich, Switzerland, 1926, pp. 332–335.

[32] O. Ozutsumi and S. Iai, "Adjustment Method of the Hysteresis Damping for Multiple Shear Spring Model," in *International Conferences on Recent Advances in Geotechnical Earthquake Engineering and Soil Dynamics*, San Diego, CA, USA, Mar. 2001.

[33] N. Mononobe and H. Matsuo, "On determination of earth pressure during earthquake," in *Proceedings of the World Engineering Congress*, Tokyo, Japan, 1929, pp. 177–185.

[34] A. Fusco, G. M. B. Viggiani, G. S. P. Madabhushi, G. Caputo, R. Conti, and C. Prüm, "Physical modelling of anchored steel sheet pile walls under seismic actions," in *Earthquake Geotechnical Engineering for Protection and Development of Environment and Constructions*, Boca Raton, FL, USA: CRC Press, 2019.